

## PRELIMINARY CHARACTERIZATION OF THE HYPERSONIC FLOW IN THE TEST SECTION OF THE IEAv T3 HYPERSONIC SHOCK TUNNEL

**Romanelli Pinto D., davidromanelli@ieav.cta.br**

**Marcos, T. V. C., thiagovcm@ieav.cta.br**

Collaborators at the Instituto de Estudos Avançados, Rod. dos Tamoios km 5,5 Putim 12.228-001 São José dos Campos, SP, Brasil  
Undergraduate students of the ETEP Faculdades (Mechanical Engineering and Physics, respectively)

**Toro, P. G. P., toro@ieav.cta.br**

**Minucci, M. A. S., sala@ieav.cta.br**

**Oliveira, A. C., acoc@ieav.cta.br**

**Chanes Junior, J. B., broslar@ieav.cta.br**

Instituto de Estudos Avançados, Rod. dos Tamoios km 5,5 Putim 12.228-001 São José dos Campos, SP, Brasil

***Abstract.** The Brazilian 14-X Hypersonic Aerospace Vehicle, designed at the Prof. Henry T. Nagamatsu Laboratory of Aerothermodynamics and Hypersonics, at the Institute for Advanced Studies (IEAv), is part of the continuing effort of the Department of Aerospace Science and Technology (DCTA), to develop a technologic demonstrator using: i) "waverider" technology to provide lift to the aerospace vehicle, and ii) "scramjet" technology to provide hypersonic airbreathing propulsion system based on supersonic combustion. The T3 0.60-m. nozzle exit diameter Hypersonic Reflected Shock Tunnel, funded by The State of São Paulo Research Foundation (FAPESP) was designed as Research & Development facility for basic investigations in supersonic combustion management. Additionally, special features were coupled in the T3 Hypersonic Shock Tunnel for experimental investigations on beamed energy laser propulsion. Finally, the T3 Hypersonic Shock Tunnel may be used for basic electromagnetic energy addition for external flow control and for general aerothermodynamics applied in conventional aerospace vehicle. The T3 Hypersonic Shock Tunnel is a shock tube fitted with a convergent-divergent nozzle to produce high Mach number and high enthalpy flows in the test section close to those encountered during the flight of a space vehicle into the Earth's atmosphere at hypersonic flight speeds. A special pitot pressure rake was designed and fabricated to house twenty nine piezoelectric pressure transducers to measure the pressure in the test section to characterize the T3 Hypersonic Shock Tunnel. Pressure distribution at the exit of the nozzle as well as schlieren photograph will be presented.*

**Keywords:** Hypersonic Shock Tunnel, Hypersonic Facility, Brazilian 14-X Hypersonic Aerospace Vehicle

### 1. INTRODUCTION

The T3 0.60-m. nozzle exit diameter Reflected Hypersonic Shock Tunnel, is new Hypersonic High Enthalpy Real Gas Pulsed Reflected Shock Tunnel, Fig. 1, funded by The State of São Paulo Research Foundation (FAPESP, process n° 2004/00525-7), and it was designed by Toro et al (2005) at the Prof. Henry T. Nagamatsu Laboratory of Aerothermodynamics and Hypersonics, at Institute for Advanced Studies (IEAv), primarily, as Research and Development (R& D) facility for basic investigations in supersonic combustion applied to high-speed advanced airbreathing propulsion.



Figure 1. T3 0.60-m. nozzle exit diameter Hypersonic Shock Tunnel.

Additionally, special features were coupled in the T3 Hypersonic Shock Tunnel for experimental investigations on beamed energy laser propulsion (Toro et al, 2007). Finally, the T3 Hypersonic Shock Tunnel may be used for basic electromagnetic energy addition for external flow control as well as for general aerothermodynamics applied in conventional aerospace vehicle.

The Brazilian 14-X Hypersonic Aerospace Vehicle, Fig. 2, designed by Rolim et al (2009) at the Prof. Henry T. Nagamatsu Laboratory of Aerothermodynamics and Hypersonics, is part of the continuing effort of the Department of Aerospace Science and Technology (DCTA), to develop a technologic demonstrator using: i) "waverider" technology to provide lift to the aerospace vehicle, and ii) "scramjet" technology to provide hypersonic airbreathing propulsion system based on supersonic combustion.

Aerospace vehicle using "waverider" technology obtains lift using the shock wave, formed during supersonic/hypersonic flight through the Earth's atmosphere, which originates at the edge and it is attached to the bottom surface of the vehicle, generating a region of high pressure, resulting in high lift and low drag. Atmospheric air, precompressed by the shock wave, which lies between the shock wave and the leading edge of the vehicle may be used in hypersonic propulsion system based on "scramjet" technology.

Hypersonic airbreathing propulsion, that uses supersonic combustion ramjet ("scramjet") technology, offers substantial advantages to improve performance of aerospace vehicle that flies at hypersonic speeds through the Earth's atmosphere, by reducing onboard fuel. Basically, scramjet is a fully integrated airbreathing aeronautical engine that uses the oblique/conical shock waves generated during the hypersonic flight, to promote compression and deceleration of freestream atmospheric air at the inlet of the scramjet. Fuel, at least sonic speed, may be injected into the supersonic airflow just downstream of the inlet. Right after, both oxygen from the atmosphere and on-board fuel are mixing. The combination of the high energies of the fuel and of the oncoming supersonic airflow the combustion at supersonic speed starts. Finally, the divergent exhaust nozzle at the afterbody vehicle accelerates the exhaust gases, creating thrust.

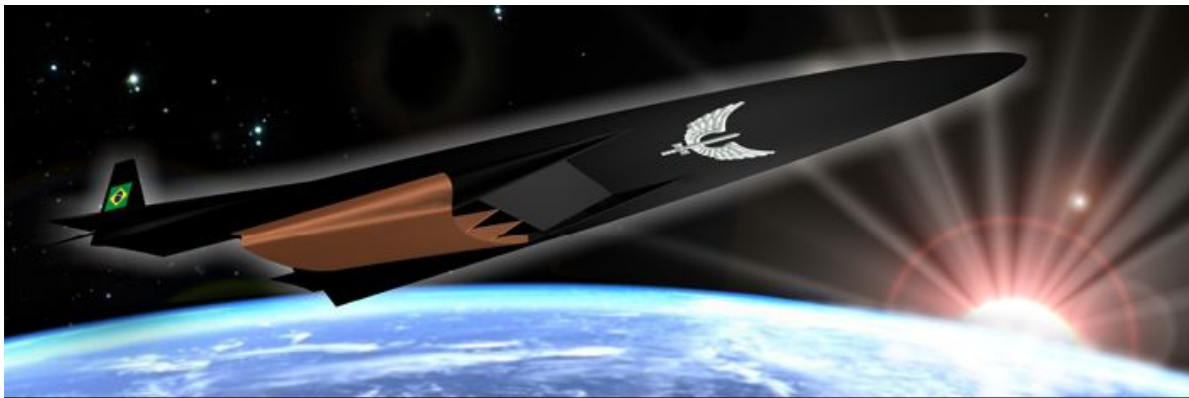


Figure 2. Brazilian 14-X Hypersonic Aerospace Vehicle.

## 2. IEAv 0.60-m. NOZZLE EXIT DIAMETER HYPERSONIC SHOCK TUNNEL

The simplest Reflected Hypersonic Shock Tunnel, Fig. 3, is a shock tube fitted with a convergent-divergent nozzle to produce high Mach number and high enthalpy flows in the test section close to those encountered during the flight of a space vehicle into the Earth's atmosphere at hypersonic flight speeds. The basic shock tunnel consists of a high-pressure (driver) section and a low-pressure (driven) section separated by a main diaphragm (DDS), a convergent-divergent nozzle and its diaphragm (attached at the end of the driven section), and a dump tank with the test section.

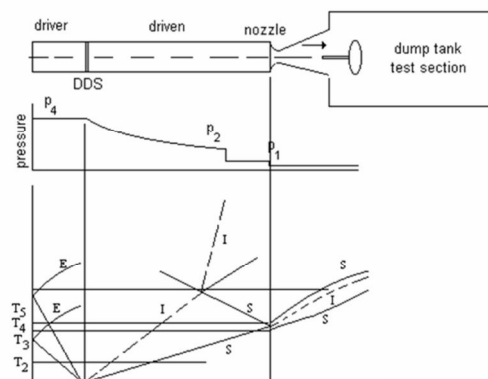


Figure 3. Schematic sketch of constant cross section area Reflected Shock Tunnel and wave diagram. (The separation between the shock wave (S) and contact surface (I) is exaggerated to show it better)

Driver-to-driven area change ( $A_4/A_1$ ), located between the driver and driven sections, is the technique used to increase shock wave strength ( $p_2/p_1$ ) for a given high driver-to-driven pressure ratio. ( $p_4/p_1$ ) (Yoler, 1958; Nagamatsu et al, 1961). Also, driver gas (helium) lighter than driven gas (air) should be used to produce higher driver-to-driven sound speed ratio ( $A_{41}=a_4/a_1$ ) and, therefore, producing strong shock waves, providing enough total temperature and Mach number, in the test section, to duplicate the high enthalpy and thermochemical characteristics close to those encountered during the flight of vehicles at high-speeds in the Earth's atmosphere. Moreover, a convergent-divergent reflected nozzle should be designed to obtain higher test time at the test section, and a minimum length ( $L_4/L_1$ ), that may be calculated using the  $L_4/L_1$  ratio constant area across the driver and driven sections (Glass and Hall, 1959).

The T3 0.60-m. nozzle exit diameter Hypersonic Shock Tunnel, Fig. 4, was designed (Toro et al, 2005) to be operated in the 6-25 flow Mach number range, generating reservoir enthalpies in excess of 10 MJ/Kg and reservoir pressures up to 25 MPa when operated in the equilibrium interface mode, with estimated useful test time of 2 ms to 10 ms. These conditions are estimated based on the driver-to-driven area ratio,  $\left(\frac{\phi_{driver}}{\phi_{driven}}\right)^2 = 2.25$ , on the driven length equal 100 times the driven internal diameter,  $\phi_{driven} = 127\text{mm}$ , and on the operating driver pressure 5000 psi. In addition, lower Mach numbers, in the range of 2.5 to 5, could be achieved in the straight through operation configuration.

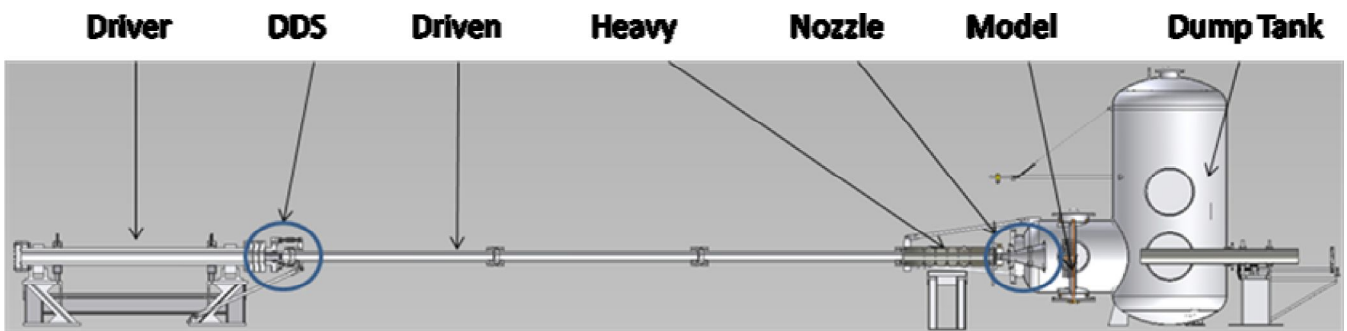


Figure 4. T3 0.60-m. nozzle exit diameter Hypersonic Shock Tunnel.

The driver section, Fig. 4, was designed with an internal diameter of 190.5-mm, and 4-m. length, with a hydraulic volume of 114 liters ( $0.114\text{ m}^3$ ). This part was machined from a forged medium carbon steel bar; the large external diameter of 305-mm permits a wall thickness of 57.25-mm. This heavy driver was designed to be operated at 35 MPa (5000 psi), at room temperature.

The Double Diaphragm Section (DDS), Fig. 4, was designed to control the exact moment of the start of the experiment. Due to the extreme weight of the driver tube (around 2,000kg), a sleeve section was designed so that the driver tube does not have to be moved during the replacement of the diaphragms. This section has also a contraction region to produce a stronger incident shock wave for the same driver-to-driven pressure ratio existing in a constant area shock tube. A third section, which will be used to operate the tunnel with the Gaseous Piston (Nascimento, 1997), is also provided. In this case, a thin section (downstream of the double diaphragm section), is pressurized with a heavy molecular weight gas to separate the driver gas from the driven gas, increasing both stagnation pressure and stagnation temperature in the Equilibrium Interface Mode of Operation.

The driven section, Fig. 4, is made from three cold rolled medium carbon steel tubes, with 3.50-m. length each and 127-mm internal diameter, used in hydraulic actuator sleeves. These tubes are easily found in the market, with the internal bore honed to achieve both high dimensional precision and a very low surface roughness. These conditions are necessary to improve the performance of the tunnel. Each tube is joined one to another with specially designed flanges, which will be fitted with openings, permitting installation of both the instrumentation and the plumbing system.

The end of the driven section consists of a heavy section, Fig. 4, 1.5-m. in length that is used to couple the throat/nozzle section to the driven section. The heavy section is fitted with 20 instrumentation ports to allow for the shock pressure, heat transfer and speed measurements needed to determine the flow conditions over the model or the experiment. The maximum operating pressure is 40 MPa. The total length of the driven tube including the transition section (DDS) and heavy-end section is 12.70-m., which is in agreement with the optimum length suggested in the literature in terms of test time.

The nozzle section was designed as a simple conical expansion section, with  $15^\circ$  half-angle and interchangeable throats, in the same way as used in the Rensselaer Polytechnic Institute (RPI)/Troy (NY) (Minucci, 1991) and in the Institute for Advanced Studies (IEAv)/Brazil (Nascimento, 1997) shock tunnels. The conical expansion section is composed by four individual pieces made out from medium carbon steel and aluminum. It starts with a 42.87 mm internal diameter forged steel conical section and ends with a 600 mm exit diameter machined aluminum block. Using a sleeve system, similar to that used in the DDS section, the change of the diaphragms and the replacement of the nozzle

throat inserts are very fast. The nozzle throat was designed and machined from high carbon steel alloy and its change is made by unscrewing the nozzle throat itself and replacing to the desired one. Four radial holes were designed to facilitate the nozzle throat change and to avoid damages to the sealing surfaces.

The dump tank (test/tank) section, Fig. 4, of the new hypersonic shock tunnel was designed to be one piece. The X-direction derivation test section has 1.4-m. internal diameter by 1.4-m. length, while the vertical tank section has an internal diameter of 1.897 meters and a total length of 4.35 meters. The internal volume of the test/tank section is about 15 m<sup>3</sup>. The tank diameter was chosen considering several features; the first one was the tank weight, which implicates in the cost of fabrication. Also the diameter and the length should meet the availability of commercial steel sheets in standard thickness, which is determined by the vacuum application. A first approach was made considering these two conditions and the volume needed for the safe tunnel operation and the optimal dimensions were found 2 meter I. D. and 15 m<sup>3</sup> volume, close to the used in the actual tank design. This volume is large enough to accommodate both the gases used in the driver and in the driven sections with the final pressure of about 1 atm above the atmospheric pressure, from maximum driver and driven tube pressures. This severe condition imposes safety aspects of operation, and the vacuum pump is kept in operation during the tunnel run.

Due to the large diameter, the reflected shock waves inside the test section/dump tank walls will occur downstream the model support, meaning clear visualization of the flow and a more reliable test condition.

Eleven access windows were added to the test section/dump tank. The first is used to attach the nozzle to the tank and is located in the horizontal derivation of the tank. The internal diameter of this window is 700 mm, large enough to accommodate all the pieces of the nozzle section in the most favorable condition. The next four windows were installed symmetrically on the sides of the horizontal derivation of the tank, and will be used as flow visualization windows. The internal bore of these four windows is 500 mm, allowing for the use of 305 mm optical glass windows. Three other windows were installed on the tank wall. One of them with 800-mm diameter will be used as an electronic feed-through for the model instrumentation. The other two windows, with the same 800-mm diameter, will be used to enable the access of operators into the dump tank. The ninth window is the vacuum inlet, placed near of the top of the tank, with an internal diameter of 300 mm. This position was chosen to prevent debris from entering the vacuum pump inlet. The tenth window is placed in the centerline of the tank. This window is used to support a specially designed sting to support longer models into the tunnel. The last window is placed at the top of the tank and will be used to allow the movement of the sting/model inside of the test/tank section. The centerline of the tunnel is placed at 1220 mm from the laboratory floor level. The design considers easy access to each section, specially where the instrumentation and plumbing will be attached.

Each section is mounted on heavy steel stands, designed to hold firmly the sections. The space between each stand is, at least, 1 meter, making the operation as comfortable as possible.

## 2.1. Reflect Hypersonic Shock Tunnel Operation

Initially, both driver and driven sections are separated by a main diaphragm, which bursts at the select high pressure in the driver tube. The driver section is filled with a driver gas, at an initial high pressure  $p_4$ , Fig. 3, and an ambient temperature  $T_4$ . The driven section is filled with a driven gas, at an initial low pressure  $p_1$ , Fig. 3, and an ambient temperature  $T_1$ . Different gases at different temperatures may be used in the driver and driven sections. Before the test starts the dump tank is evacuated, with a pressure level  $p_d$ , several orders of magnitude lower than the pressure level at the driven section  $p_1$ . Driven section and dump tank are separated by a thin diaphragm to avoid the inflow of the test gas into the dump tank before the test starts.

When the main diaphragm, which separates the driver and driven gases, breaks, the unsteady one-dimensional strong normal shock wave is initiated. The shock wave is no longer constrained, and it propagates through space to the low pressure region (downstream driven section) with a propagation velocity  $u_s$ . In this case, all properties of the flowfield depend on both space ( $x$ ) and time ( $t$ ), i.e.,  $p(x,t)$ ,  $\rho(x,t)$ ,  $T(x,t)$ ,  $u(x,t)$ .

When the main diaphragm, which bursts at the selected high pressure in the driver section, opens compression waves, which steepen rapidly into a shock wave, move into a low pressure region (driven section), and compresses it to a pressure  $p_2$  at temperature  $T_2$ , and induces a mass motion with velocity,  $u_2$ . In the same running time, an expansion wave propagates upstream into a high pressure region (driver section), reducing, smoothly and continuously, the pressure from the initial values  $p_4$  and  $T_4$  to  $p_2$  and  $T_2$ . Ideal diaphragm opening and ideal wave behavior should be assumed (no damping, no viscous boundary layer effects). Behind the primary shock wave, a contact surface, which separates the driven gas and the gas from the driver, propagates downstream in the driven section. Across the contact surface, the velocity and the pressure are equal, but the temperature and the density may not be, in general, equal for both driven and driver gases. After opening the main diaphragm, the flowfield in the section is completely determined by a given condition in the driver and in the driven sections, Fig. 4, before the main diaphragm is broken, and perfect gas may be assumed for relatively low temperatures. For high temperatures, where the perfect gas is no longer valid, the real gas effects modify the results for shock tube flow.

A few milliseconds after the bursting of the main diaphragm, the primary shock wave arrives at the end wall of the driven section. In this time, the thin diaphragm, which separates the driven gas and the dump tank gas, bursts and the nozzle flow starts.

A high enthalpy shock tunnel may operate in the Reflected Shock Wave Mode or in the Equilibrium Interface Model (Minucci, 1991). The stagnation conditions may be generated, either after the primary reflected shock wave (Reflected Shock Wave Mode) or after a few shock wave reflections (Equilibrium Interface Mode) from the shock section end wall and the approaching contact surface, due to the relatively small nozzle throat diameter, then propagates upstream. Right after the first reflection process, the thin diaphragm between driven section and nozzle bursts and the nozzle flow starts. The compressed test gas expands through the nozzle and the gas with high stagnation enthalpy is converted into a free stream of high velocity in the test section. Also, for longer test times the Reflected Mode can be achieved by tailoring the contact surface, however this method is restricted by the choice of the different pressure-temperature combinations.

The stagnation conditions for the hypersonic flow over the model in the test section are generated after the reflected shock wave (Reflected Mode) or after several contact surface intersections (Equilibrium Interface Mode) produced in the end wall of the shock tube (driven section). As a consequence, the correct modeling of the shock tunnel flow phenomena is of great importance.

The instantaneous rupture of the diaphragms, the establishment of the shock wave right after the rupture of the diaphragms, and no formation of the viscous boundary layer on the shock tube wall are assumed in the governing flow equations. Unfortunately, the diaphragms are ruptured in a finite time and the shock wave is formed over a length of several tube diameters. Also, the viscous boundary layer is built up on the shock tube wall. Because of these factors the shock wave strength is decreased and the shock wave Mach number is less than the one computed from the pressure ratio across the diaphragms.

No ideal opening of the diaphragm and viscous effects cause the incident shock wave to reach a lower terminal flow velocity than that predicted by the ideal perfect gas theory. Also, these two effects cause the contact surface to spread and to accelerate. The real gas effects (caloric imperfections, dissociation, ionization) usually tend to lower the reflected temperature, and to increase the stagnation pressure (Minucci, 1991).

High Mach number and high stagnation temperature flows are characterized by the phenomena of vibration and dissociation of molecules and ionization of atoms and molecules. Experimental hypersonic flow investigations (Minucci, 1991) show that there exist two distinct situations: low and high enthalpy conditions. The low enthalpy case may be modeled by a calorically or thermally perfect gas, while the model of a mixture of the gases in thermodynamic equilibrium must be used to study the high enthalpy case. In a calorically perfect gas the specific heats,  $c_p$  and  $c_v$ , are considered constant. A thermally perfect gas is one in which the specific heats are functions of only the temperature. This is a result of the vibrational energy within the gas molecules and the electronic energy associated with the electron motion within the atoms or molecules. In both cases the perfect gas equation of state may be used. In the more general case of a purely compressible gas at thermodynamic equilibrium, the specific heats are functions of two thermodynamic properties, for example the pressure and the temperature. The real gas equation of state should be used for such cases.

For high enthalpy stagnation conditions, the Reflected Mode operation is presented. In this mode of operation, the incident shock wave is reflected from the shock tube end wall (or nozzle entrance), and the conditions existing between the first reflected shock wave and the end wall constitute the stagnation conditions for the model in the test section.

## 2.2. Reflect Hypersonic Shock Tunnel Flow Modeling

The governing flow equations for the one-dimensional incident shock wave (Figs. 3 and 5) are given by

$$\text{continuity: } \rho_1 u_s = \rho_2 (u_s - u_2) \quad (1)$$

$$\text{momentum: } p_1 + \rho_1 u_s^2 = p_2 + \rho_2 (u_s - u_2)^2 \quad (2)$$

$$\text{energy: } h_1 + \frac{1}{2} u_s^2 = h_2 + \frac{1}{2} (u_s - u_2)^2 \quad (3)$$

$$\text{equation of state: } h_2 = h_2(p_2, \rho_2) \quad (4)$$

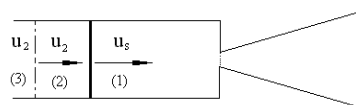


Figure 5. Incident Shock Wave.

Once the conditions after the incident shock wave are determined, the conditions existing between the reflected shock wave and the nozzle entrance must be found. Due to the presence of the nozzle throat, the incident shock wave is only partially reflected and the transmitted shock wave disrupts the flow in the nozzle. As a consequence, there exists a

finite subsonic velocity  $u_5$  imparted to the flow between the reflected wave and the nozzle inlet. The choked flow at the nozzle throat is assumed.

The governing flow equations for the one-dimensional reflected shock wave with reflected nozzle (Fig. 3 and 6) are given for reflected shock wave flow by

$$\text{continuity: } \rho_2(u_2 + u_r) = \rho_5(u_r + u_5) \quad (5)$$

$$\text{momentum: } p_2 + \rho_2(u_2 + u_r)^2 = p_5 + \rho_5(u_r + u_5)^2 \quad (6)$$

$$\text{energy: } h_2 + \frac{1}{2}(u_2 + u_r)^2 = h_5 + \frac{1}{2}(u_r + u_5)^2 \quad (7)$$

$$\text{equation of state: } h_5 = h_5(p_5, \rho_5) \quad (8)$$

and for nozzle throat flow by

$$\text{continuity: } \rho_5 u_5 A_t = \rho^* a^* A^* \quad (9)$$

$$\text{momentum: } p_5 + \rho_5 u_5^2 = p^* + \rho^* (a^*)^2 \quad (10)$$

$$\text{energy: } h_5 + \frac{1}{2}u_5^2 = h^* + \frac{1}{2}(a^*)^2 \quad (11)$$

$$\text{equation of state: } h^* = h^*(p^*, \rho^*) \quad (12)$$

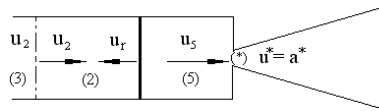


Figure 6. Reflected Shock Wave and Nozzle Entrance.

Once the conditions existing between the first reflected shock wave and the end wall are determined, the stagnation conditions for the model in the test section can be found by the flow in the nozzle in thermodynamic equilibrium, Fig. 7.

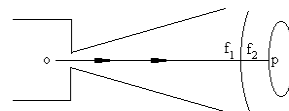


Figure 7. Nozzle Flow.

The flow in the nozzle of the T3 0.60-m. nozzle exit diameter Reflected Hypersonic Shock Tunnel may be assumed in thermodynamic equilibrium for reservoir temperature of 4500K and reservoir pressure exceeding 500 psi (Nagamatsu et al, 1960; Nagamatsu et al, 1961; Nagamatsu and Sheer, 1965). Since the flow expands in the nozzle, the bow normal shock wave is formed in front of the body nose, which is located on the nozzle centerline. The flow in the nozzle expansion is accelerated (upstream) and the flow over the body is decelerated (downstream). In both cases the flow is adiabatic (short duration flow) and isentropic (thermodynamic equilibrium). The flow across the bow shock wave is adiabatic but not isentropic. The inviscid (no boundary layer on the nozzle wall) one-dimensional conservation laws may be used, and they are given by

$$\text{continuity: } \rho_{f1} u_{f1} = \rho_{f2} u_{f2} \quad (13)$$

$$\text{momentum: } p_{f1} + \rho_{f1} u_{f1}^2 = p_{f2} + \rho_{f2} u_{f2}^2 \quad (14)$$

$$\text{energy: } h_{f1} + \frac{1}{2}u_{f1}^2 = h_{f2} + \frac{1}{2}u_{f2}^2 \quad (15)$$

$$\text{equation of state: } h = h(p, \rho) \quad (16)$$

Since the energy is conserved along the streamline, through the shock wave, it may be rewritten as

$$\text{energy: } h_{f1} + \frac{1}{2}u_{f1}^2 = h_{f2} + \frac{1}{2}u_{f2}^2 = h_o \quad (17)$$

and in addition, the isentropic flow upstream (in the nozzle expansion) and downstream (ahead) of shock wave are, respectively, given by,

$$s_{f1} = s_o \tag{18}$$

$$s_{f2} = s_p \tag{19}$$

In thermodynamic equilibrium flow two thermodynamic variables determine the gas state.  $s_o$  can be determined from the stagnation (reservoir) conditions  $h_o$  and  $p_o$ , which are known from the shock tunnel flow modeling  $h_5$  and  $p_5$ .  $s_p$  can be determined from the flow at stagnation point of the body, the enthalpy by equation 2.17 and the pressure, which is experimentally measured by pitot probe.

The equilibrium thermodynamic properties, at high enthalpy stagnation condition, are calculated from real gas equation of state. Minucci (1991) presents the solution for this problem with real gas effects for air. The real gas effects are taken into account by utilizing the tabulated real air properties given by Tannehill and Mugge (1974). For calorically perfect gas, low enthalpy stagnation condition, the non-linear system of equations produce analytical algebraic equations as a function only of Mach number of the shock wave and the properties upstream of the shock wave. Nagamatsu et al (1961), Anderson (1990) and John (1984) among many others, present the equations and analyses for this case. Also, Anderson (1990) and John (1984) solved the incident shock wave with real gas by iterative process.

Minucci (1991) presented not only the flow modeling for both cases, the Reflected Shock Wave Mode and the Equilibrium Interface Mode, but he also developed a CFD code to solve the equations.

### 2.3. Flow Visualization Schlieren Technique

An ultra high-speed camera, manufactured by CORDIN, model 550, coupled with mirror-based schlieren ‘Z’ configuration, Fig. 8 (left) was used for dynamic flow visualization. This Schlieren system is composed of a pulsed xenon flash lamp, an optical slit and focusing lens, two parabolic and three flat mirrors, the knife edge which provides the necessary light cut-off to the Cordin 550 ultra-high speed camera. Also, Fig. 8 (right) shows the schlieren light beam path and placement of the Cordin camera, with respect to the T3 Hypersonic Shock Tunnel test section.

The Cordin 550 camera acquires 32 frames with a maximum resolution of 1000 x 1000 pixels at up to 2 million frames per second (fps) in full color. Such frame rates are achieved by a multi-faceted mirror spinning at high speeds, surrounded by 32 CCD elements which acquire images as the mirror rotates. Mirror rotation is driven by a turbine wheel supplied with high pressure  $N_2$  for frame rates up to 500,000 fps, and pressurized He for the highest speeds. Even though extremely high speeds can be achieved, the present work demanded more modest 50,000 to 100,000 fps.

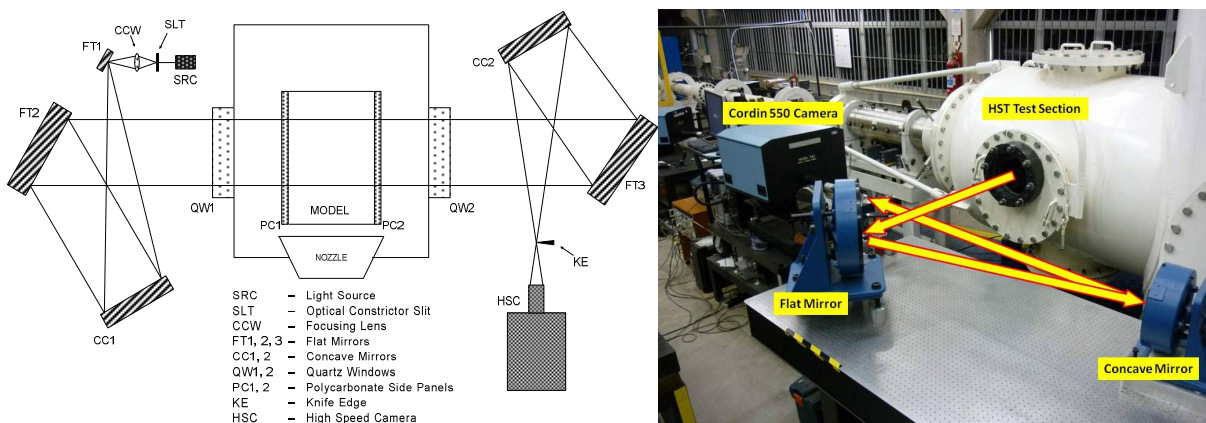


Figure 8. (Left) Schlieren visualization and high speed Cordin 550 camera system setup and (right) schlieren light beam path and placement of the speed Cordin 550 camera.

A multichannel time-delay generator is used to synchronize all the equipment used in the experiment (data acquisition system, and schlieren system) within the useful shock-tunnel time. The unit was triggered by a Kistler piezoelectric pressure transducer (model 701 A) located immediately upstream of the nozzle entrance. Also, this transducer supplies the reservoir pressure of the nozzle. Two other Kistler 701A transducers, located 0.314-m. apart at the end of the tunnel-driven section, mounted flush with the shock tube (heavy section) inner wall, were used to time the incident shock wave.

### 3. TEST SECTION FLOW CHARACTERIZATION

The subsonic-supersonic (hypersonic) isentropic flow through variable-area ducts (convergent-divergent nozzle) may be used to determine the flow at the nozzle exit (Anderson, 1990), which will be establish the hypersonic flow in the test section, Fig. 9.

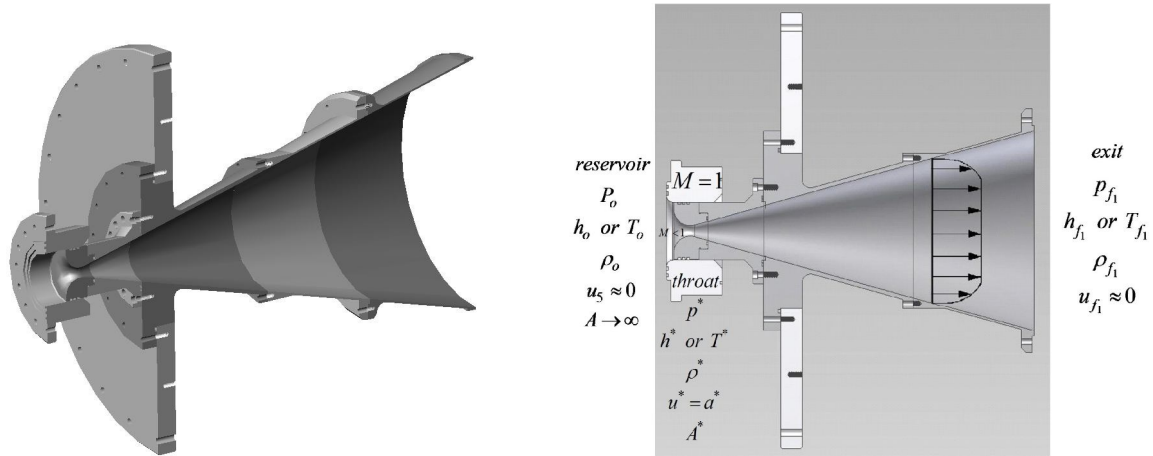


Figure 9. Schematic for subsonic-supersonic (hypersonic) isentropic flow through variable-area ducts (convergent-divergent nozzle).

The flow at the inlet of the nozzle comes from the compressed test gas (from the driven section, reservoir, of the T3 Hypersonic Shock Tunnel). The flow expands isentropically to supersonic (hypersonic) speeds at the nozzle exit, and the high stagnation enthalpy of the oncoming flow is converted into a freestream high speeds in the test section.

To verify the uniformity of the hypersonic flow in the test section of the T3 Hypersonic Shock Tunnel, a special pitot pressure rake, Fig. 10, was fabricated to house twenty-nine (29) piezoelectric pressure transducers.

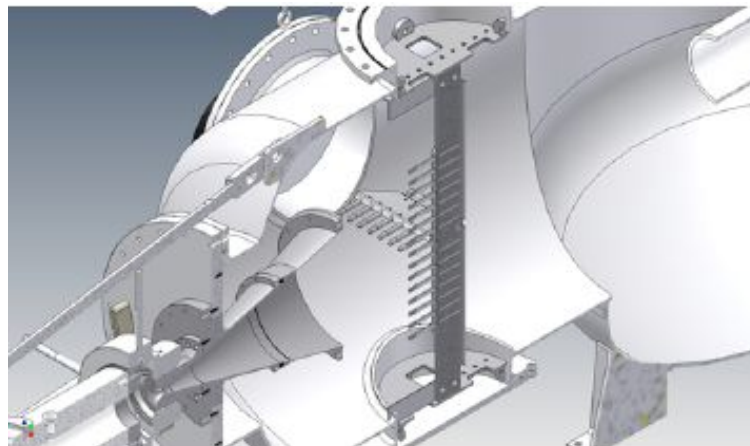


Figure 10. Schematic view of the pitot pressure rake mounted in the test section of the T3 Hypersonic Shock Tunnel.

#### 4. HYPERSONIC FLOW MACH 10 NOZZLE PERFORMANCE

The T3 0.60-m. nozzle exit diameter Hypersonic Shock Tunnel, Fig. 1, used to conduct the Experimental Investigation of Hypersonic Flow Characterization, is capable of generating both high to low enthalpy hypersonic flow conditions. In the present investigation, of high enthalpy runs, helium is used as the driver gas and the tunnel operates in the equilibrium interface condition to produce a useful test time of roughly 1 ms. The test section airflow Mach number is 9.16 in the high enthalpy tests. The conical, 15° half angle and 600 mm exit diameter, nozzle with a throat diameter of 26.35 mm is used in all Mach number 9.16 runs.

Figure 11 display typical pressure traces for the present investigation for high enthalpy air conditions. The first two traces (from left) measure the time of the incident shock wave in the driven section. The third trace measures the reservoir pressure, and the fourth the impact pressure (pitot pressure).

The Schlieren photograph, Fig. 12, of Mach number 9.16 flow over a “pitot pressure” at the pitot pressure rake, shows that the shock is symmetrical, and the experimental stand-off distance of  $\delta = 1.04 \text{ mm}$ , Fig. 12, agrees with the estimate (12%) given by the correlation of Billing (1967)  $\delta = 1.18 \text{ mm}$ , which is based on experimental data given by:

$$\frac{\delta}{R} = 0.143 \exp\left(\frac{3.24}{M_\infty^2}\right) \quad (20)$$

where R is the radius of the nose of the pitot pressure model and  $M_\infty$  is the Mach number of undisturbed flow.

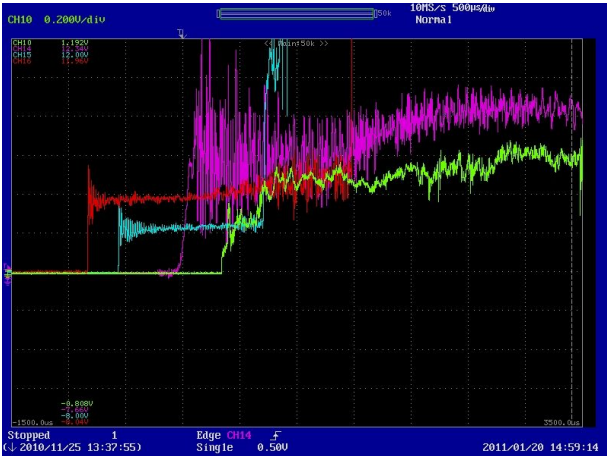


Figure 11. Typical pressure traces (voltage trace) for the present investigation.

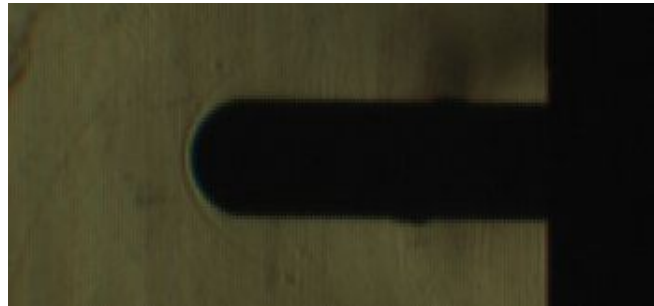


Figure 12. Schlieren photograph of the pitot pressure of the pitot pressure rake.

The pressure distribution, Fig. 13, of hypersonic Mach number 9.16 flow at the pitot pressure rake at the exit of the nozzle, shows that the shock is symmetrical. The boundary layer is in between the external circle (pressure transducers 1, 13, 7, 8) and the internal circle (pressure transducers 2, 12, 6, 9). More data between both circles to clear the position of the boundary layer is needed.

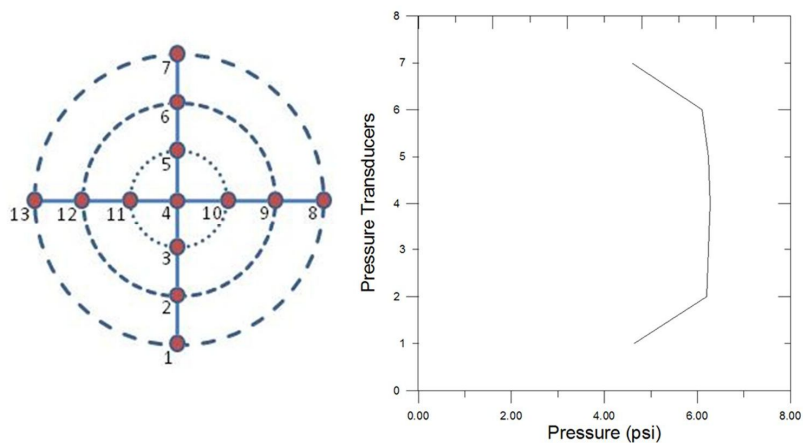


Figure 13. Pressure measurements at the nozzle exit for Mach number 9.16.

Also, time-lapse photography, of the luminous air flow around the semi-spherical model, Fig. 14, takes by a Nikon D-1H (digital camera) with AF24-120mm f/3.5-f/5.6 Nikkor lenses, shows the flow is symmetrical.

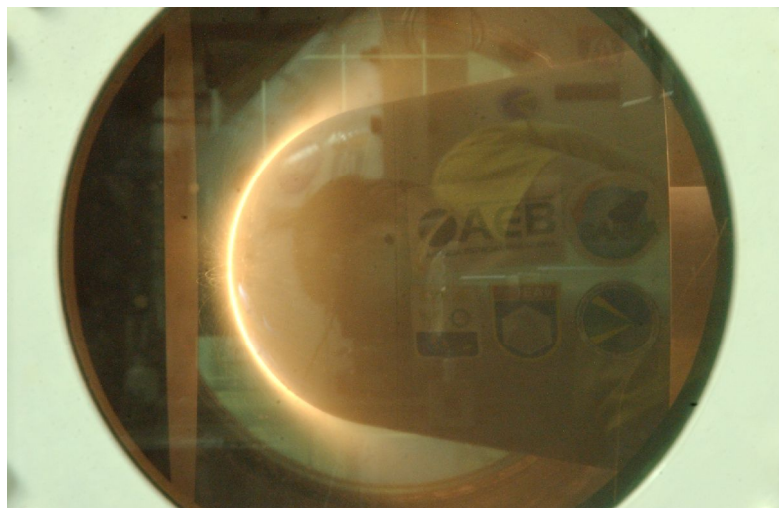


Figure 14. Time-lapse photography of the Mach 10 air flow.

## 5. CONCLUSION

The T3 0.60-m. nozzle exit diameter Reflected Hypersonic Shock Tunnel, is new Hypersonic High Enthalpy Real Gas Pulsed Reflected Shock Tunnel, funded by The State of São Paulo Research Foundation (FAPESP), and it was designed at the Prof. Henry T. Nagamatsu Laboratory of Aerothermodynamics and Hypersonics, at Institute for Advanced Studies (IEAv), primarily, as Research and Development facility for basic investigations in supersonic combustion applied to high-speed advanced airbreathing propulsion. The Brazilian 14-X Hypersonic Aerospace Vehicle, designed at the Prof. Henry T. Nagamatsu Laboratory of Aerothermodynamics and Hypersonics, is part of the continuing effort of the Department of Aerospace Science and Technology (DCTA), to develop a technologic demonstrator using: i) "waverider" technology to provide lift to the aerospace vehicle, and ii) "scramjet" technology to provide hypersonic airbreathing propulsion system based on supersonic combustion.

Special pitot pressure rake was fabricated to house twenty-nine piezoelectric pressure transducers, to measure the pressure in the test section to characterize the uniformity of the hypersonic flow in the test section of the T3 Hypersonic Shock Tunnel. Pressure distributions at the exit of the nozzle as well as schlieren photography shows the hypersonic flow at the nozzle exit is symmetrical.

## 6. ACKNOWLEDGEMENTS

The third author would like to express his gratitude to the Financiadora de Estudos e Projetos (FINEP, project nº 0445/07, grant # 01.08.0365.00) and Conselho Nacional de Desenvolvimento Científico e Tecnológico (CNPq, process nº 520017/2009-9) their continued support. Also, acknowledgment is due to the CNPq for the financial support of the two first authors (grant # 380821/2009-5 and grant # 380823/2009-8, respectively). Special thanks are due to Arthur Freire Mantovani, Renan Guilherme Santos Vilela, Victor Alves Barros Galvão, José Adeildo dos Santos Assenção and Felipe Jean da Costa (CNPq grants: # 181294/2010-9, # 183244/2009-5, # 183691/2009-1, # 183240/2009-0 and # 183245/2009-1, respectively) for their help in the IEAv T3 Hypersonic Shock Tunnel operation.

## 7. REFERENCES

- Anderson Jr., J. A., 1990, "Modern Compressible Flow, The Historical Perspective" McGraw-Hill, Inc., 2<sup>nd</sup> edition.
- Glass, I.I. and Hall, J.G., 1959, "Shock Tubes". Handbook of Supersonic Aerodynamics, section 18. Navord Report 1488 (vol. 6).
- John, E. A. J., 1984, "Gas Dynamics," Allyn and Bacon, Inc, 2<sup>nd</sup> edition.
- Minucci, M.A.S. 1991, "An Experimental Investigation of a 2-D Scramjet Inlet at Flow Mach Numbers of 8 to 25 and Stagnation Temperatures of 800 to 4100 K," Ph.D. Thesis, Rensselaer Polytechnic Institute, New York.
- Nagamatsu, H.T., Geiger, R.E. and Sheer Jr., R.E., 1960, "Real Gas Effects in Flow over Blunt Bodies at Hypersonic Flow," J. of the Aero/Space Sciences, vol. 27, no. 4.
- Nagamatsu, H.T., Workman, J.B. and Sheer, R.E., Jr., 1961, "Hypersonic Nozzle Expansion of Air with Atom Recombination Present," J. of the Aero/Space Sciences, vol. 28, n. 11, pp. 833-837.
- Nagamatsu, H.T. and Sheer, R.E., Jr., 1965, "Vibration Relaxation and Recombination of Nitrogen and Air in Hypersonic Flows," AIAA Journal, vol. 3, n. 8, pp. 1386-1391.
- Nascimento, M.A.C., 1997, "Gaseous Piston Effect in Shock Tube/Tunnel When Operating in the Equilibrium Interface Condition," Doctoral Thesis, Instituto Tecnológico de Aeronáutica - ITA, Divisão de Engenharia Aeronáutica, São José dos Campos, SP, Brazil.
- Tannehill, J. C.; Mugee, P. H., 1974, "Improved Curve Fits for the Thermodynamic Properties of Equilibrium suitable for Numerical Computation using Time-Dependent or Shock-Capturing Methods," NASA CR 2470.
- Rolim, T.C., Minucci, M.A.S, Toro, P.G.P, Soviero, P.A.O, 2009, "Experimental Results of a Mach 10 Conical-Flow Derived Waverider", Proceedings of the 16<sup>th</sup> AIAA/DLR/DGLR International Space Planes and Hypersonic Systems and Technologies Conference, Bremen, Germany. (AIAA-2009-7433).
- Yoler, Y.A., 1954, "Hypersonic Shock Tube," California Institute of technology, GALCIT.
- Toro, P. G. P., Minucci, M. A. S., Chanes Jr., J. B., Pereira, A. L. and Nagamatsu, H. T., 2005, "Development of a New Hypersonic Shock Tunnel Facility to Investigate basic Supersonic Combustion and basic Electromagnetic Energy Addition for Flow Control". 4<sup>th</sup> International Symposium on Beamed Energy Propulsion, Japan.
- Toro, P. G. P., Minucci, M. A. S., Chanes Jr., J. B., Oliveira, A.C., Gomes, F. A. A., Myrabo, L. N., and Nagamatsu, H. T. (*in Memoriam*), 2007, "New Hypersonic Shock Tunnel at the Laboratory of Aerothermodynamics and Hypersonics Prof. Henry T. Nagamatsu", 4<sup>th</sup> International Symposium on Beamed Energy Propulsion, Hawaii.

## 8. RESPONSIBILITY NOTICE

The authors are the only responsible for the printed material included in this paper.

Copyright ©2011 by P. G. P. Toro. Published by the 21<sup>st</sup> Brazilian Congress of Mechanical Engineering (COBEM).